

ORGANIC CHEMISTRY FRONTIERS

RESEARCH ARTICLE

[View Article Online](#)
[View Journal](#) | [View Issue](#)



Cite this: *Org. Chem. Front.*, 2021, **8**, 1117

Sequence-controlled supramolecular copolymer constructed by self-sorting assembly of multiple noncovalent interactions†

Hui Li, *^a Ying Yang, ^a Fenfen Xu, ^a Zhaozhao Duan, ^a Riqiang Li, ^a Herui Wen^a and Wei Tian *^b

In this work, four monomers, M1, M2, M3, and M4, were designed and synthesized. M1 + M2 + M3 + M4 + Zn(OTf)₂ could self-assemble into a sequence-controlled supramolecular copolymer through self-sorting at relatively high concentrations. The self-sorting assembly of the four monomers was verified by NMR spectroscopy, UV-Vis spectroscopy, viscosity measurements, dynamic light scattering, fluorescence spectroscopy, SEM, and TEM analyses. The experimental results showed that supramolecular polymerization depended on the initial concentrations of the monomers. The resulting supramolecular copolymer (**SCP**) showed K⁺ responsiveness, and adding-removing K⁺ could drive the disassembly-reassembly of SCP. Moreover, OH⁻ could enhance the fluorescence emission of the SCP-based solution or film. The SCP could also be applied to prepare honeycomb-patterned films. With stimuli-responsive behavior and regulatable fluorescence properties, the SCP has potential application value in creating smart adaptive materials.

Received 9th December 2020,
Accepted 27th January 2021

DOI: 10.1039/d0qo01540g
rsc.li/frontiers-organic

Introduction

Biopolymers in nature possess unique functions that are associated with their precisely defined structure sequences. Engineering the monomer sequence of a polymer main chain is a considerable challenge in conventional polymer synthesis.^{1,2} Supramolecular polymerization offers another approach for developing sequence-controlled polymer chains.^{3,4} With the development of supramolecular science, a variety of methodologies have been developed to prepare sophisticated supramolecular structures.⁵⁻⁸ Among these methodologies, self-sorting assembly is an important method and has been developed to control the sequence of monomer arrays in supramolecular copolymerization.⁹ Self-sorting was proposed to describe the capability of molecules in a mixture to selectively find their counterparts and form specific pairs rather than binding randomly.^{9,10} Self-sorting is the outcome of competing recognition behavior through the binding constants among all possible pairs, and high specificity is required for

each binding event. Many interactions or factors including steric effects, coordination spheres, charge transfers, sizes and shapes can drive a self-sorting process.¹¹⁻²⁶ By means of self-sorting assembly, various delicate supramolecular architectures, including sequence-controlled supramolecular polymers, can be easily constructed.¹¹⁻²⁶ Huang and Wang reported a supramolecular copolymer based on self-sorting assembly of double crown ethers-based host-guest recognitions.²⁷ Alternatively, Haino *et al.* prepared a sequence-controlled supramolecular polymer through self-sorting assembly of complementary calix[5]arene-C60, bisporphyrin-TNF, and Hamilton's complexes, which provided possibilities for constructing advanced functional polymers with tailored sequences.²⁸

Metal coordination, as one kind of directional and strong supramolecular force, has been widely adopted to construct precisely defined supramolecular structures.²⁹⁻³² Through rational molecule design, diverse metal coordination interactions have been developed.³³⁻³⁵ It was found that terpyridine (**tpy**) and its derivative 6,6''-anthracyl-substituted tpy (**tay**) can form a complementary ligand pair, and the ligand pair can form a heteroleptic complex tpy-M-tay with metal ions in solution.³⁶ Compared to the homoleptic tpy-M-tpy complex, the heteroleptic tpy-M-tay structure is more stable due to the enhanced π - π stacking interactions between the anthracene moieties and the tpy group. On the other hand, host-guest interactions, as another kind of supramolecular force, are

^aSchool of Metallurgical and Chemical Engineering, Jiangxi University of Science and Technology, Ganzhou 341000, P. R. China. E-mail: lh@jxust.edu.cn

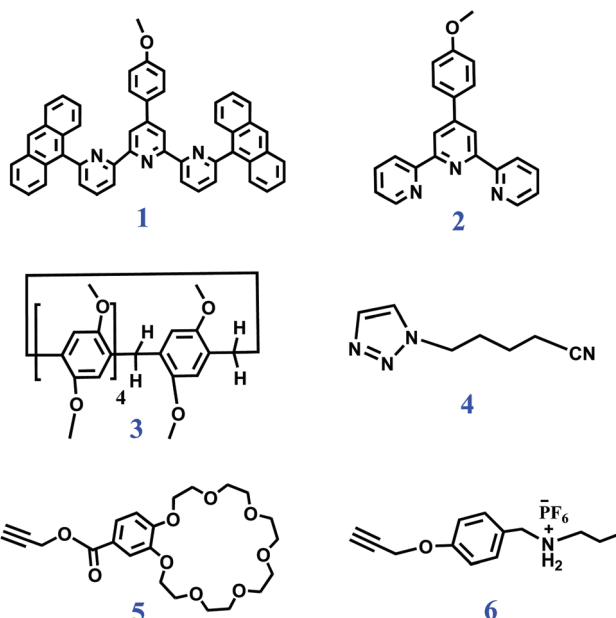
^bShaanxi Key Laboratory of Macromolecular Science and Technology, School of Science, Northwestern Polytechnical University, Xi'an 710072, P. R. China.
E-mail: happytw_3000@nwpu.edu.cn

† Electronic supplementary information (ESI) available. See DOI: 10.1039/d0qo01540g

important research branches of supramolecular chemistry. Macrocycle hosts such as crown ethers and pillararenes are well known to efficiently bind guest molecules for fabricating supramolecular assemblies, which provide unique physical and chemical properties for obtaining interlocked species.^{37–44} Although various supramolecular polymers prepared through metal coordination, crown ether- and pillararene-based host-guest recognitions have been reported, the fabrication of supramolecular polymers by combining the three noncovalent reactions has not been reported before. If the involved metal coordination, pillararene-based host-guest interaction, and crown ether-based host-guest interaction are proved to be self-sorting in a system, a sequence-controlled supramolecular polymer fabricated *via* self-sorting assembly of the three noncovalent interactions will hopefully be prepared. Herein, we synthesized four monomers as follows. Heteroditopic **M1** consists of a tpy and a neutral guest (**TPN**); heteroditopic **M2** bears a tay group and a crown ether group (**B21C7**); homoditopic **M3** contains two pillar[5]arene (**P5**) groups; and homoditopic **M4** consists of two dialkylammonium salt (**SEA**) moieties. A mixture of **M1** + **M2** + **M3** + **M4** + $Zn(O Tf)_2$ was expected to form a sequence-controlled supramolecular copolymer (**SCP**) by self-sorting assembly at relatively high concentrations (Scheme 1).

Results and discussion

To investigate the self-sorting binding process, six model molecules **1**–**6** were first synthesized (Scheme 2). First, a sequence

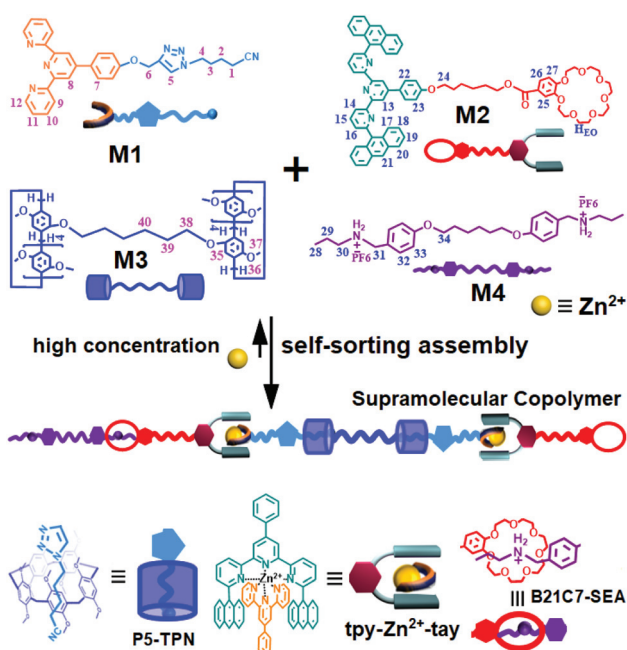


Scheme 2 Chemical structures of the model compounds **1**–**6**.

of samples comprising two model molecules were prepared, and the 1H NMR spectra of the samples were collected (Fig. S1–S5, ESI†). When equimolar **1**, **2**, and $Zn(O Tf)_2$ were dissolved in $CDCl_3$ – CD_3COCD_3 (3 : 1, v/v), 1H NMR peak shifts were observed, verifying that the complementary tpy and tay ligands spontaneously formed the heteroleptic complex tpy- Zn^{2+} -tay in the presence of Zn^{2+} ions (Fig. S1†).³⁶ When **3** and equimolar **4** were mixed together in $CDCl_3$ – CD_3COCD_3 , the 1H NMR spectrum clearly showed the binding of P5-TPN (Fig. S2†). The host-guest interaction of **5** and **6** was also investigated, and a complex 1H NMR spectrum revealed the slow exchange interaction between B21C7 and SEA (Fig. S3†).⁴¹ On the other hand, the 1H NMR spectra also showed that pillar[5] arene could not bind to the secondary ammonium salt in $CDCl_3$ – CD_3COCD_3 (Fig. S4†), and B21C7 could not bind to TPN (Fig. S5†).

The self-sorting complexation among different model compounds in $CDCl_3$ – CD_3COCD_3 was then studied. A sequence of samples comprising two different noncovalent interactions were prepared. The 1H NMR spectra clearly showed self-sorting complexation between P5-TPN and tpy- Zn^{2+} -tay (Fig. S6†), between B21C7-SEA and tpy- Zn^{2+} -tay (Fig. S7†), and between B21C7-SEA and P5-TPN (Fig. S8†). Finally, the 1H NMR spectrum of equimolar **1** + **2** + **3** + **4** + **5** + **6** + $Zn(O Tf)_2$ in $CDCl_3$ – CD_3COCD_3 clearly showed that self-sorting complexation indeed occurred. That is, in a $CDCl_3$ – CD_3COCD_3 solution of **1** + **2** + **3** + **4** + **5** + **6** + $Zn(O Tf)_2$, **1** binds **2** in the presence of zinc ions, **3** binds **4**, and **4** binds **5** (Fig. S9†).

We then mixed **M1** + **M2** + **M3** + **M4** + $Zn(O Tf)_2$ together (molar ratio: 2 : 2 : 1 : 1 : 2) in a $CDCl_3$ – CD_3COCD_3 (3 : 1, v/v) solution and investigated whether they could form supramolecular copolymers by self-sorting assembly. The 1H NMR spectrum of **M1** + **M2** + **M3** + **M4** + $Zn(O Tf)_2$ (Fig. 1e) was compli-



Scheme 1 Schematic illustration of the supramolecular copolymer **SCP** constructed from the monomers **M1** + **M2** + **M3** + **M4** + Zn^{2+} by self-sorting assembly.

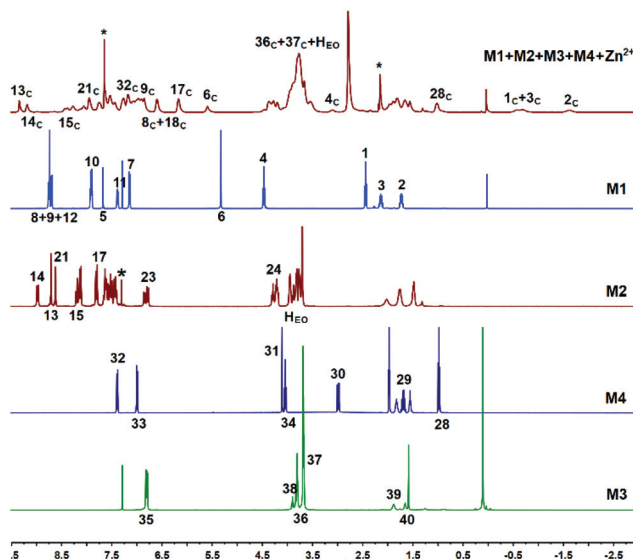


Fig. 1 ^1H NMR (400 MHz, chloroform- d_3 /acetone- d_6 , 293 K) spectra of (a) M3, (b) M4, (c) M2, (d) M1, and (e) a mixture of M1 + M2 + M3 + M4 + Zn(OTf)₂ at a 10 mM concentration (molar ratio: M1 : M2 : M3 : M4 : Zn(OTf)₂ = 2 : 2 : 1 : 1 : 2). The peaks of the complexed monomers were designated as c.

cated due to the coexistence of multiple noncovalent interactions. By comparison with the ^1H NMR spectra of the model molecules (Fig. S1–S6[†]) and the help of the COSY NMR spectrum (Fig. S10[†]), the complex ^1H NMR spectrum of M1 + M2 + M3 + M4 + Zn(OTf)₂ was interpreted. At a low concentration, H_{1–4} on M1 shifted upfield, indicating that the alkyl moiety of M1 threaded into the hole of P5 of M3.⁴⁴ Meanwhile, proton H₃₂ of M4 shifted upfield, and proton H₃₀ shifted downfield, which implies the occurrence of the binding interaction B21C7-SEA.⁴¹ Furthermore, protons H_{8–9} of M1 shifted upfield, and protons H_{13–15} shifted downfield, verifying the formation of metal ligand coordination tpy-Zn²⁺-tay.³⁶ The ^1H NMR spectrum of M1 + M2 + M3 + M4 + Zn(OTf)₂ clearly revealed that self-sorting assembly among the four monomers indeed occurred, as illustrated by the analysis of the model molecules. NOESY NMR analysis was then performed to further study the self-sorting assembly. The strong correlations between H_{1–4} from M1 and H_{35–37} from M3 indicated that the TPN moiety of M1 thrust into the hole of M3 (Fig. 2). Correlations between H_{30,32} of M4 and H_{EO} of M2 were also observed, indicating that the B21C7 moiety of M2 tightly bound the SEA moiety of M4 in the mixed solvent.⁴¹

Furthermore, UV-Vis titration was also conducted to study the self-sorting assembly. The titration experiment was first carried out by adding Zn(OTf)₂ to the solution of M1 + M2 (Fig. 3a), and the titration plots showed an isosbestic point at 311 nm, suggesting the gradual transformation from the free tpy and tay moieties to a metal-ligand coordination species.⁴⁵ A maximum absorbance of 346 nm was observed when the molar ratio reached 1 : 1 : 1 (Zn²⁺ : M1 : M2), which further confirmed the formation of the tpy-Zn²⁺-tay structure. The titra-

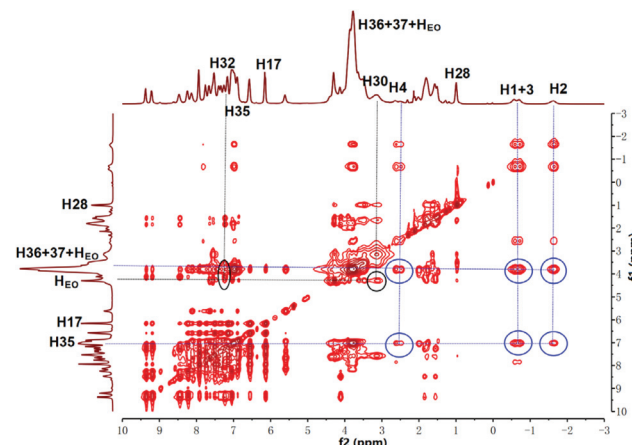


Fig. 2 NOESY NMR (400 MHz, CDCl₃–CD₃COCD₃ = 3/1, v/v, 298 K) spectrum of M1 + M2 + M3 + M4 + Zn(OTf)₂.

tion curves of M1 + M2 + M3 + M4 + Zn(OTf)₂ were similar to the curves of M1 + M2 + Zn(OTf)₂ (Fig. 3b), and an endpoint was observed when the molar ratio was 2 : 2 : 2 : 1 : 1 (M1 : M2 : Zn(OTf)₂ : M3 : M4), suggesting that B21C7-SEA and P5-TPN host–guest interactions did not interfere with the tpy-Zn²⁺-tay coordination. The above UV-Vis titration further verified the self-sorting assembly among the four monomers. Finally, the concentration-dependent ^1H NMR spectra revealed that increasing the concentration of monomers could broaden the ^1H NMR spectra (Fig. S11, ESI[†]), which implied the formation of supramolecular copolymer SCP at high concentrations.

Diffusion-ordered NMR spectroscopy was also carried out to investigate the self-sorting assembly. When the concentration of monomers changed from 2 to 130 mM (Fig. 4a and Fig. S12[†]), the diffusion coefficient (D) for the solution of M1 + M2 + M3 + M4 + Zn(OTf)₂ decreased significantly from 5.56×10^{-10} to $4.21 \times 10^{-11} \text{ m}^2 \text{ s}^{-1}$ ($D_{2.0} \text{ mM}/D_{130.0} \text{ mM} = 13$), indicating that supramolecular polymerization of M1 + M2 + M3 + M4 + Zn(OTf)₂ was concentration-dependent. According to the concentration-dependent property of supramolecular polymerization,^{46,47} a high polymerization degree required that the D value be reduced more than 10 times. The experimental D value supported that the supramolecular copolymer was stepwise generated from the small oligomer to the supramolecular polymer when the monomer concentrations increased. Capillary viscosity was also measured to study the formation of SCP. A bilogarithmic graph of specific viscosity against the concentration of monomer is plotted in Fig. 4b. A curve slope of 0.93 was observed at low concentrations, implying the predominance of oligomers at low concentrations.⁴⁴ However, the curve slope became 1.75 at a relatively high concentration (the critical polymerization concentration value is approximately 28 mM), indicative of a gradual transition from small oligomers to larger supramolecular copolymers. The formation of supramolecular copolymer SCP at high concentration was further verified by SEM observation (Fig. 4c). A rod-

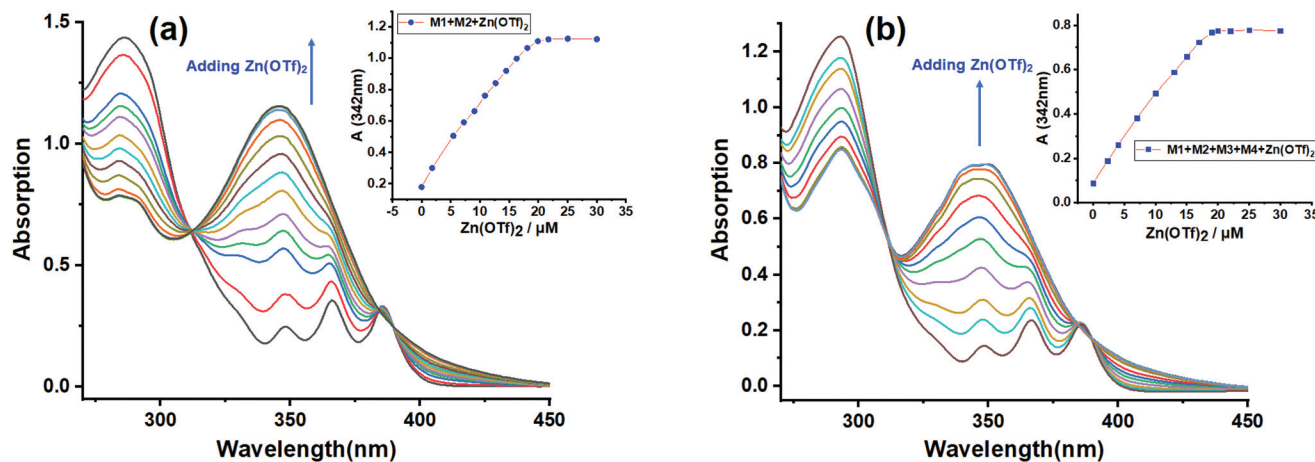


Fig. 3 (a) Changes in UV-Vis absorption after gradually adding $\text{Zn}(\text{OTf})_2$ to a 0.02 mM $\text{M}1 + \text{M}2$ solution; (b) changes in UV-Vis absorption after gradually adding $\text{Zn}(\text{OTf})_2$ to a 0.02 mM $\text{M}1 + \text{M}2 + \text{M}3 + \text{M}4$ solution. Inset: the changes in absorption intensity at 342 nm.

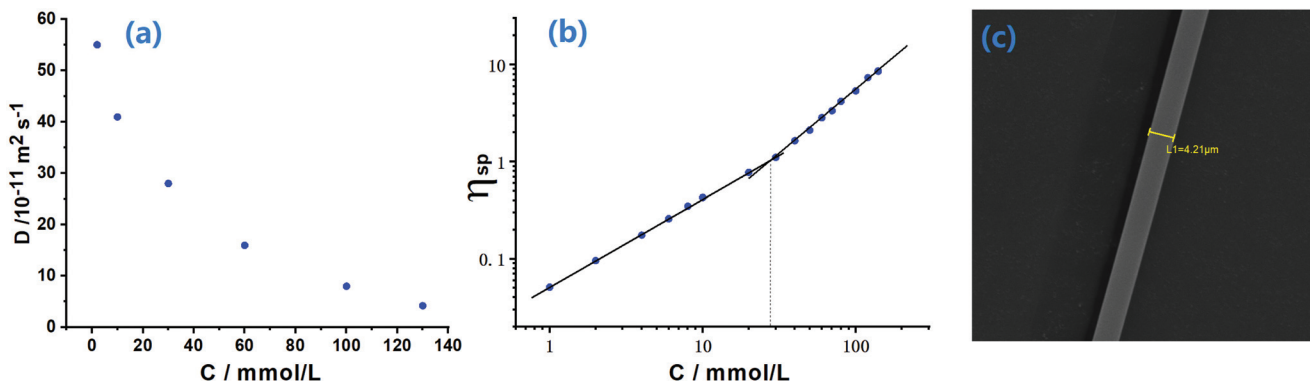


Fig. 4 (a) Diffusion coefficient of $\text{M}1 + \text{M}2 + \text{M}3 + \text{M}4 + \text{Zn}(\text{OTf})_2$ against the concentration of $\text{M}1$ (600 MHz, 293 K); (b) specific viscosity of $\text{M}1 + \text{M}2 + \text{M}3 + \text{M}4 + \text{Zn}(\text{OTf})_2$ against the concentration of $\text{M}1$. Molar ratio: $\text{M}1 : \text{M}2 : \text{M}3 : \text{M}4 : \text{Zn}(\text{OTf})_2 = 2 : 2 : 1 : 1 : 2$; (c) SEM image of a rodlike fiber drawn from a highly concentrated solution of $\text{M}1 + \text{M}2 + \text{M}3 + \text{M}4 + \text{Zn}(\text{OTf})_2$.

like fiber could be drawn from a highly concentrated solution of $\text{M}1 + \text{M}2 + \text{M}3 + \text{M}4 + \text{Zn}(\text{OTf})_2$. The fibers provided direct evidence of the formation of supramolecular copolymers SCP at high concentrations.²⁷ The high viscosity of the SCP solution at high concentration was an important factor for extension of the fiber under the drawing of an external force.

DLS (dynamic light scattering) and TEM were then adopted to observe the size of the SCP in solution and the morphology of the SCP at dry state. The $\text{CHCl}_3-\text{CH}_3\text{COCH}_3$ solution of $\text{M}1 + \text{M}2 + \text{M}3 + \text{M}4 + \text{Zn}(\text{OTf})_2$ showed an average hydrodynamic diameter (D_h) of 160 nm (Fig. 5a, $[\text{M}1] = 120$ mM). In contrast, no large aggregate was observed for the 10 mM solution, verifying the concentration dependence of the supramolecular polymerization. The morphology of the supramolecular copolymer SCP was then observed by TEM. The TEM photograph of the SCP showed a spherical morphology (Fig. 5b). It should be noted that the TEM may be difficult to accurately measure the size of SCP due to the dynamics of noncovalent bonds and the existence of the secondary assembly when the SCP was removed from the solution to dry state.⁴⁸ Because monomers

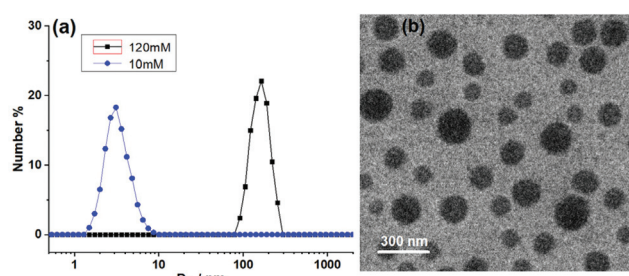


Fig. 5 (a) The hydrodynamic diameter distribution of $\text{M}1 + \text{M}2 + \text{M}3 + \text{M}4 + \text{Zn}(\text{OTf})_2$ in $\text{CHCl}_3-\text{CH}_3\text{COCH}_3$ (3 : 1, v/v, $\text{M}1 = 120$ mM or 10 mM, molar ratio: $\text{M}1 : \text{M}2 : \text{M}3 : \text{M}4 : \text{Zn}(\text{OTf})_2 = 2 : 2 : 1 : 1 : 2$, 293 K); (b) representative TEM image of $\text{M}1 + \text{M}2 + \text{M}3 + \text{M}4 + \text{Zn}(\text{OTf})_2$.

$\text{M}2$, $\text{M}3$, and $\text{M}4$ have very flexible chains of six methylene groups, the globular morphology may be a result of the entanglement of the linear supramolecular copolymer SCP.⁴⁴ To confirm that the spherical morphology visualized by TEM was derived from the supramolecular copolymer, control experi-

ments were performed for ternary mixtures lacking one of the building blocks. No spherical morphology could be observed in $M1 + M2 + M3 + \text{Zn}(\text{OTf})_2$, $M2 + M3 + M4 + \text{Zn}(\text{OTf})_2$, or $M1 + M2 + M4 + \text{Zn}(\text{OTf})_2$ solutions. This phenomenon indicated that the self-sorting assembly among the four monomers was crucial for the formation of SCP.

Next, we studied the stimuli-responsiveness of SCP. Because B21C7 can capture K^+ ,⁴¹ adding-removing K^+ could realize the reversible disassembly-reassembly of SCP (Fig. S15 and 16, ESI†). On the other hand, butanedinitrile could also induce the disassembly of SCP by destroying the binding of P5-TPN (Fig. S17, ESI†). In addition to the B21C7-SEA and P5-TPN host-guest interactions that could be manipulated, we speculated that tpy-Zn²⁺-tay binding could also be adjusted by removing the Zn²⁺ ions.⁴⁹ A thin yellow film was fabricated by spouting the solution of the SCP onto one glass, which was then dried in air. The yellow-green film fabricated by SCP gave off almost no fluorescence under the illumination of a 365 nm UV lamp. However, when tBAOH was added into the film, the film emitted blue fluorescence (Fig. 6a). This phenomenon could be explained as shown below: adding tBAOH into the film caused the generation of zinc hydroxide, which resulted in breakage of the tpy-Zn²⁺-tay coordination structure and induced the removal of Zn²⁺ from the skeleton of SCP. The removal of Zn²⁺ drove the disassembly of SCP and induced the coordinative tay moiety into a free tay moiety. The free tay moiety emitted blue fluorescence under UV lamp irradiation because of the existence of two anthracene chromophores on the free tay moiety. The fluorescence emission spectra supported this inference (Fig. S19, ESI†). A similar fluorescence emission enhancement was observed when adding tBAOH to the solution of SCP (Fig. 6b).

Finally, the SCP was tested to determine whether it could be applied to fabricate 2D honeycomb films, which have potential value in adsorption, separation, and catalysis.^{50,51} By means of a breath figure method (BF), a well-organized honeycomb film was prepared from the SCP-based solution. The diameters of these pores were approximately $1 \pm 0.5 \mu\text{m}$ through

SEM observation (Fig. 6c). Usually, honeycomb structures fabricated *via* the BF method need a certain segment density,^{52–54} which could facilitate polymer settling around water droplets. The entangled polymer chain of SCP constructed by self-sorting assembly and the increasing viscosity are speculated to stabilize the water droplets when the solvent is evaporated, generating an ordered microstructure after the water was totally removed.

Conclusions

In summary, four monomers, M1, M2, M3, and M4, were designed and synthesized. $M1 + M2 + M3 + M4 + \text{Zn}(\text{OTf})_2$ could self-assemble into a sequence-controlled supramolecular copolymer SCP through self-sorting at relatively high concentrations. The self-sorting binding among the three different noncovalent interactions, P5-TPN, B21C7-SEA, and tpy-Zn²⁺-tay, and the self-sorting assembly among the four monomers were verified by a combination of NMR spectroscopy, UV-Vis spectroscopy, viscosity measurements, dynamic light scattering, SEM, TEM, and fluorescence spectroscopy. The experiments also verified that the supramolecular polymerization depended on the initial concentrations of the monomers. The resulting supramolecular copolymer SCP showed K^+ and butanedinitrile responsiveness, and adding-removing K^+ could drive the disassembly-reassembly of the SCP. Moreover, OH[−] could induce the fluorescence emission enhancement of the SCP-based solution or film. The SCP could also be applied to prepare honeycomb films. With stimuli-responsive behavior and regulatable fluorescence properties, SCP possesses potential value in creating smart adaptive materials.

Experimental

Materials and methods

The synthetic routes and characterizations of monomers M2 and M3 were afforded in the ESI.† Monomers M1,²³ M4,¹⁹ and some intermediate compounds 7,³⁶ 9,⁵⁵ were synthesized according to the literatures. The other reagents and solvents were either employed as purchased or dried prior to use by usual laboratory methods. Column chromatography was performed on silica gel (200–300 mesh). All reactions were carried out in atmosphere unless noted. ¹H NMR, ¹³C NMR, ¹H-¹H COSY, NOESY experiments were recorded on a Bruker AVANCE III 400 MHz spectrometer. Viscosity measurements were carried out with Ubbelohde micro viscometers (0.40 mm inner diameter) at 298 K in chloroform-acetone (3/1, v/v). The two-dimensional diffusion-ordered NMR (DOSY) spectra were recorded on a Bruker DRX600 spectrometer. High-resolution electrospray ionization mass spectra (HR-ESI-MS) were obtained on a Bruker Esquire 3000 plus mass spectrometer. MALDI-TOF-MASS spectrometry was performed on an AXIMA-CFR plus mass spectrometer. Dynamic light scattering (DLS) measurements were carried out on a Brookhaven

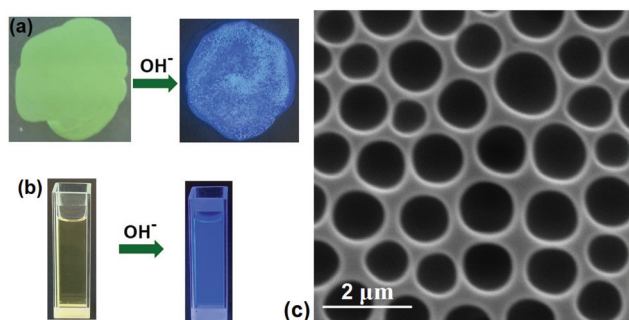


Fig. 6 (a) Images of a SCP-based film and the TBAOH responsiveness of the film; (b) images of the SCP-based solution and fluorescence change by adding TBAOH to the solution; (c) the SEM image of the porous film.

BI-9000AT system (Brookhaven Instruments Corporation, USA). UV-Vis absorption spectrum was recorded on a PerkinElmer Lambda 35 UV/vis spectrometer. Fluorescence spectra were collected on a Shimadzu RF-5301PC spectrofluorometer.

The TEM samples were conducted at a 100 mM concentration, a drop of sample solution (chloroform/acetone = 3/1, v/v) was placed on a carbon-coated copper grid. After the solvent was removed in a short time, TEM images were taken on a JEM-2100 instrument.

The honeycomb film was prepared by a breath figure method: a $\text{CDCl}_3\text{-CD}_3\text{COCD}_3$ (3:1, v/v) solution of M1 + M2 + M3 + M4 + $\text{Zn}(\text{OTf})_2$ (molar ratio: 2:2:1:1:2) was prepared at a concentration of 6.5 wt% to obtain a SCP solution. Next, 30 μL of the prepared SCP solution was dropped onto a treated PET substrate using a syringe. A steady moist nitrogen flowed through the surface of the SCP solution. After the solvent and water were evaporated thoroughly, an ordered honeycomb film was formed on the surface of PET substrate. The honeycomb film was then observed on a JEOL 6390LV scanning electron microscopy (SEM) instrument, and the sample of film was sprayed with conductive coating before being taken.

Conflicts of interest

The authors declare no conflict of interest.

Acknowledgements

This work was supported by the National Natural Science Foundation of China (Grant No. 21801100, 22022107, 22071197), the Natural Science Foundation of Jiangxi Province (20192BAB213014), the Program of Qingjiang Excellent Young Talents, Jiangxi University of Science and Technology, and Natural Science Basic Research Plan in Shaanxi Province of China (2020JC-20).

Notes and references

- 1 J. F. Lutz, M. Ouchi, D. Liu and M. Sawamoto, Sequence-controlled polymers, *Science*, 2013, **341**, 1238149.
- 2 J. F. Lutz, J. M. Lehn, E. W. Meijer and K. Matyjaszewski, From precision polymers to complex materials and systems, *Nat. Rev. Mater.*, 2016, **1**, 16024.
- 3 X. Shi, X. Zhang, X. Ni, H. Zhang, P. Wei, J. Liu, H. Xing, H. Peng, J. W. Y. Lam, P. Zhang, Z. Wang, H. Hao and B. Tang, Supramolecular Polymerization with Dynamic Self-Sorting Sequence Control, *Macromolecules*, 2019, **52**, 8814–8825.
- 4 T. Haino, Molecular-recognition-directed formation of supramolecular polymers, *Polym. J.*, 2013, **45**, 363–383.
- 5 M. L. Saha, S. De, S. Pramanik and M. Schmittel, Orthogonality in discrete self-assembly – survey of current concepts, *Chem. Soc. Rev.*, 2013, **42**, 6860–6909.

- 6 A. Wu and L. Isaacs, Self-Sorting: The Exception or the Rule?, *J. Am. Chem. Soc.*, 2003, **125**, 4831–4835.
- 7 L. Chen and H. Yang, Construction of Stimuli-Responsive Functional Materials via Hierarchical Self-Assembly Involving Coordination Interactions, *Acc. Chem. Res.*, 2018, **51**, 2699–2710.
- 8 D. Xia, P. Wang, X. Ji, N. M. Khashab, J. L. Sessler and F. Huang, Functional Supramolecular Polymeric Networks: The Marriage of Covalent Polymers and Macrocyclic-Based Host–Guest Interactions, *Chem. Rev.*, 2020, **120**, 6070–6123.
- 9 M. M. S. Sempere, G. Fernandez and F. Wurthner, Self-Sorting Phenomena in Complex Supramolecular Systems, *Chem. Rev.*, 2011, **111**, 5784–5581.
- 10 Z. He, W. Jiang and C. A. Schalley, Integrative self-sorting: a versatile strategy for the construction of complex supramolecular architecture, *Chem. Soc. Rev.*, 2015, **44**, 779–789.
- 11 H. Barbero, N. A. Thompson and E. Masson, “Dual Layer” Self-Sorting with Cucurbiturils, *J. Am. Chem. Soc.*, 2020, **142**, 867–873.
- 12 W. Jiang, H. D. F. Winkler and C. A. Schalley, Integrative Self-Sorting: Construction of a Cascade-Stoppered Hetero[3]rotaxane, *J. Am. Chem. Soc.*, 2008, **130**, 13852–13853.
- 13 H. Li, Y. Han, Y. Lin, Z. Guo and G. Jin, Stepwise Construction of Discrete Heterometallic Coordination Cages Based on Self-Sorting Strategy, *J. Am. Chem. Soc.*, 2014, **136**, 2982–2985.
- 14 N. Tomimasu, A. Kanaya, Y. Takashima, H. Yamaguchi and A. Harada, Social Self-Sorting: Alternating Supramolecular Oligomer Consisting of Isomers, *J. Am. Chem. Soc.*, 2009, **131**, 12339–12343.
- 15 Y. Wang, M. Lovrak, Q. Liu, C. Maity, V. A. A. Sage, X. Guo, R. Eelkema and J. H. V. Esch, Hierarchically Compartmentalized Supramolecular Gels through Multilevel Self-Sorting, *J. Am. Chem. Soc.*, 2019, **141**, 2847–2851.
- 16 S. Rao, Q. Zhang, J. Mei, X. Ye, C. Gao, Q. Wang, D. Qu and H. Tian, One-pot synthesis of hetero[6]rotaxane bearing three different kinds of macrocycle through a self-sorting process, *Chem. Sci.*, 2017, **8**, 6777–6783.
- 17 Z. Huang, L. Yang, Y. Liu, Z. Wang, O. Scherman and X. Zhang, Supramolecular Polymerization Promoted and Controlled through Self-Sorting, *Angew. Chem., Int. Ed.*, 2014, **53**, 5351–5355.
- 18 J. Zhong, L. Zhang, D. P. August, G. F. S. Whitehead and D. A. Leigh, Self-Sorting Assembly of Molecular Trefoil Knots of Single Handedness, *J. Am. Chem. Soc.*, 2019, **141**, 14249–14256.
- 19 R. Li, W. Chen, Y. Yang, H. Li, F. Xu, Z. Duan, T. Liang, H. Wen and W. Tian, Architecture transition of supramolecular polymers through hierarchical self-assembly: from supramolecular polymers to fluorescent materials, *Polym. Chem.*, 2020, **11**, 5642–5648.
- 20 J. F. Ayme, J. E. Beves, C. J. Campbell and D. A. Leigh, The Self-Sorting Behavior of Circular Helicates and Molecular Knots and Links, *Angew. Chem., Int. Ed.*, 2014, **53**, 7823–7827.

21 M. L. Saha and M. Schmittel, From 3-Fold Completive Self-Sorting of a Nine-Component Library to a Seven-Component Scalene Quadrilateral, *J. Am. Chem. Soc.*, 2013, **135**, 17743–17746.

22 M. L. Pellizzaro, K. A. Houton and A. J. Wilson, Sequential and phototriggered supramolecular self-sorting cascades using hydrogen-bonded motifs, *Chem. Sci.*, 2013, **4**, 1825–1829.

23 H. Li, W. Chen, F. Xu, X. Fan, T. Liang, X. Qi and W. Tian, A Color-Tunable Fluorescent Supramolecular Hyperbranched Polymer Constructed by Pillar[5]arene-Based Host–Guest Recognition and Metal Ion Coordination Interaction, *Macromol. Rapid Commun.*, 2018, **39**, 1800053.

24 Y. Yang, X. Ni, J. Xu and X. Zhang, Fabrication of nor-seco-Cucurbit[10]uril Based Supramolecular Polymers via Self-Sorting, *Chem. Commun.*, 2019, **55**, 13836–13839.

25 W. Wang, Y. Zhang, B. Sun, L. Chen, X. Xu, M. Wang, X. Li, Y. Yu, W. Jiang and H. Yang, The construction of complex multicomponent supramolecular systems via the combination of orthogonal self-assembly and the self-sorting approach, *Chem. Sci.*, 2014, **5**, 4554–4560.

26 S. Dong, X. Yan, B. Zheng, J. Chen, X. Ding, Y. Yu, D. Xu, M. Zhang and F. Huang, A Supramolecular Polymer Blend Containing Two Different Supramolecular Polymers through Self-Sorting Organization of Two Heteroditopic Monomers, *Chem. – Eur. J.*, 2012, **18**, 4195–4199.

27 F. Wang, C. Han, C. He, Q. Zhou, J. Zhang, C. Li, N. Wang and F. Huang, Self-Sorting Organization of Two Heteroditopic Monomers to Supramolecular Alternating Copolymers, *J. Am. Chem. Soc.*, 2008, **130**, 11254–11255.

28 T. Hirao, H. Kudo, T. Amimoto and T. Haino, Sequence-controlled supramolecular terpolymerization directed by specific molecular recognitions, *Nat. Commun.*, 2017, **8**, 634.

29 Q. Zhang, D. Tang, J. Zhang, R. Ni, L. Xu, T. He, X. Lin, X. Li, H. Qiu, S. Yin and P. J. Stang, Self-Healing Heterometallic Supramolecular Polymers Constructed by Hierarchical Assembly of Triply Orthogonal Interactions with Tunable Photophysical Properties, *J. Am. Chem. Soc.*, 2019, **141**, 17909–17917.

30 A. Winter and U. S. Schubert, Synthesis and characterization of metallo-supramolecular polymers, *Chem. Soc. Rev.*, 2016, **45**, 5311–5357.

31 P. Wei, X. Yan and F. Huang, Supramolecular polymers constructed by orthogonal self-assembly based on host–guest and metal–ligand interactions, *Chem. Soc. Rev.*, 2015, **44**, 815–832.

32 X. Yan, T. R. Cook, P. Wang, F. Huang and P. J. Stang, Highly emissive platinum(II) metallacages, *Nat. Chem.*, 2015, **7**, 342–348.

33 K. C. Bentz and S. M. Cohen, Supramolecular Metallopolymers: From Linear Materials to Infinite Networks, *Angew. Chem., Int. Ed.*, 2018, **57**, 14992–15001.

34 C. Lu, M. Zhang, D. Tang, X. Yan, Z. Zhang, Z. Zhou, B. Song, H. Wang, X. Li, S. Yin, H. Sepehrpour and P. J. Stang, Fluorescent Metallacage-Core Supramolecular Polymer Gel Formed by Orthogonal Metal Coordination and Host–Guest Interactions, *J. Am. Chem. Soc.*, 2018, **140**, 7674–7680.

35 J. Yan, H. Huang, Z. Miao, Q. Zhang and Y. Yan, Polyoxometalate-Based Hybrid Supramolecular Polymer via Orthogonal Metal Coordination and Reversible Photo-Cross-Linking, *Macromolecules*, 2019, **52**, 9545–9554.

36 Y. He, T. Tu, M. Su, C. Yang, K. Kong and Y. Chan, Facile Construction of Metallo-Supramolecular P3HTb-PEO Diblock Copolymers via Complementary Coordination and Their Self-Assembled Nanostructures, *J. Am. Chem. Soc.*, 2017, **139**, 4218–4224.

37 T. Ogoshi, T. A. Yamagishi and Y. Nakamoto, Pillar-Shaped Macrocyclic Hosts Pillar[n]arenes: New Key Players for Supramolecular Chemistry, *Chem. Rev.*, 2016, **116**, 7937–8002.

38 K. Jie, Y. Zhou, E. Li and F. Huang, Nonporous Adaptive Crystals of Pillararenes, *Acc. Chem. Res.*, 2018, **51**, 2064–2072.

39 N. Song, T. Kakuta, T. A. Yamagishi, Y. Yang and T. Ogoshi, Molecular-Scale Porous Materials Based on Pillar[n]arenes, *Chem.*, 2018, **4**, 2029–2053.

40 B. Zheng, F. Wang, S. Dong and F. Huang, Supramolecular polymers constructed by crown ether-based molecular recognition, *Chem. Soc. Rev.*, 2012, **41**, 1621–1636.

41 C. Zhang, S. Li, J. Zhang, K. Zhu, N. Li and F. Huang, Benzo-21-Crown-7/Secondary Dialkylammonium Salt [2]Pseudorotaxane- and [2]Rotaxane-Type Threaded Structures, *Org. Lett.*, 2007, **9**, 5553–5556.

42 H. Li, Z. Duan, Y. Yang, F. Xu, M. Chen, T. Liang, Y. Bai and R. Li, Regulable Aggregation-Induced Emission Supramolecular Polymer and Gel Based on Self-sorting Assembly, *Macromolecules*, 2020, **53**, 4255–4263.

43 Z. Zhang, Y. Liu, J. Zhao and X. Yan, Engineering orthogonality in the construction of an alternating rhomboidal copolymer with high fidelity via integrative self-sorting, *Polym. Chem.*, 2020, **11**, 367–374.

44 C. Li, K. Han, J. Li, Y. Zhang, W. Chen, Y. Yu and X. Jia, Supramolecular Polymers Based on Efficient Pillar[5]arene—Neutral Guest Motifs, *Chem. – Eur. J.*, 2013, **19**, 11892–11897.

45 Y. Ding, P. Wang, Y. Tian, Y. Tian and F. Wang, Formation of stimuli-responsive supramolecular polymeric assemblies via orthogonal metal–ligand and host–guest interactions, *Chem. Commun.*, 2013, **49**, 5951–5953.

46 S. Dong, Y. Luo, X. Yan, B. Zheng, X. Ding, Y. Yu, Z. Ma, Q. Zhao and F. Huang, A Dual-Responsive Supramolecular Polymer Gel Formed by Crown Ether Based Molecular Recognition, *Angew. Chem., Int. Ed.*, 2011, **50**, 1905–1909.

47 Z. Li, Y. Y. Zhang, C. Zhang, L. Chen, C. Wang, H. Tan, Y. Yu, X. Li and H. Yang, Cross-Linked Supramolecular Polymer Gels Constructed from Discrete Multi-pillar[5]arene Metallacycles and Their Multiple Stimuli-Responsive Behavior, *J. Am. Chem. Soc.*, 2014, **136**, 8577–8589.

48 T. Liu, S. Wang, Y. Song, J. Li, H. X. Yana and W. Tian, *Polym. Chem.*, 2017, **8**, 1306–1314.

49 B. Shi, K. Jie, Y. Zhou, D. Xia and Y. Yao, Formation of fluorescent supramolecular polymeric assemblies via orthogonal pillar[5]arene-based molecular recognition and metal ion coordination, *Chem. Commun.*, 2015, **51**, 4503–4506.

50 I. Tokarev and S. Minko, Multiresponsive, Hierarchically Structured Membranes: New, Challenging, Biomimetic Materials for Biosensors, Controlled Release, Biochemical Gates, and Nanoreactors, *Adv. Mater.*, 2009, **21**, 241–247.

51 C. Ma, Y. Zhong, J. Li, C. Chen, J. Gong, S. Xie, L. Li and Z. Ma, Patterned Carbon Nanotubes with Adjustable Array: A Functional Breath Figure Approach, *Chem. Mater.*, 2010, **22**, 2367–2374.

52 U. H. F. Bunz, Breath Figures as a Dynamic Templating Method for Polymers and Nanomaterials, *Adv. Mater.*, 2006, **18**, 973–989.

53 M. J. Kim, Y. Yu, C. G. Chae, H. B. Seo and J. S. Lee, Facile Synthesis of Amphiphilic Bottlebrush Block Copolymers Bearing Pyridine Pendants via Click Reaction from Protected Alkyne Side Groups, *Macromolecules*, 2020, **53**, 2209–2219.

54 J. Li, J. Dong, K. Cui, H. Wang, Y. Sun, Y. Yao, J. Chen, J. Gu and S. Lin, Pillararene-based supramolecular membranes with the rose-petal effect and nanostructure-modulated tunable water adhesion, *J. Mater. Chem. A*, 2020, **8**, 10917–10924.

55 T. Ogoshi, T. Aoki, K. Kitajima, S. Fujinami, T. Yamagishi and Y. Nakamoto, Facile, Rapid, and High-Yield Synthesis of Pillar[5]arene from Commercially Available Reagents and Its X-ray Crystal Structure, *J. Org. Chem.*, 2011, **76**, 328–331.